The Portability of Some Regional Seismic Discriminants And Related Broadband Waveform Modeling

Bradley B. Woods and Chandan K. Saikia
Woodward-Clyde Federal Services,
Pasadena, CA

F49620-94-C-0046
Sponsored by AFOSR

ABSTRACT

We are investigating the portability of regional seismic discriminants which were developed from the analysis of data for southwestern U.S. earthquakes and NTS explosions. Besides determining whether or not these discriminants are effective for seismic events in other tectonically active regions, it will be possible to calibrate the effective discriminant parameters for these different regions, so that an event from any such area can be incorporated into a unified database. Events studied are the U.S. PNE's and earthquakes in the Colorado Plateau/Rockies region, explosions at the Kazakh (CIS) and Lop Nor (PRC) test sites, as well as earthquakes in and around this region of Asia. Events in Pakistan are analyzed by these discriminants, too, although no explosion data are available. This region includes significant deep seismicity (d>50km). The discriminants being used here are the ratio of integrated short-period P-wave to long-period energy (predominantly surface wave) summed over the three components (sp_z-P/lp_3) (Woods and Helmberger, 1994), the ratio of integrated short-period vertical component energy between the P and S wavetrains (sp_z-P/sp_z-S), and the ratio of M_L to scalar seismic moment (M_0). For the Colorado Plateau data set the energy ratio discriminants were modified to use peak amplitudes, as many of the records could not be digitized. The sp_z-P/lp_3 discriminant is most effective at distinguishing source-types. The sp_z-P/sp_z-S energy ratio appears to be useful to identify deep events from shallower crustal earthquakes. The M_L:M_0 discriminant is deterministic, requiring Green's functions that reflect the crustal structure of a region with which to invert waveform data to obtain the source parameters for any event. To this end we have modeled broadband regional records at WMQ and those recorded by the PASCAL array in Pakistan. Initial modeling of the Pakistan region has been successful using a thick crustal model developed for the Tibetan Plateau. Well-constrained source mechanisms have been obtained for deep and shallow events. One potential use of regional waveform modeling in areas of deep seismicity is to calibrate t^* for teleseismic m_b measurements. Once the source parameters and source time function are determined by regional source inversion, then teleseismic body-waves can be fit by varying Q in the mantle source region.

OBJECTIVE:

We are investigating the portability of regional seismic discriminants which were developed from the analysis of data for southwestern U.S. earthquakes and NTS explosions. Besides determining whether or not these discriminants are effective for seismic events in other tectonically active regions, it will be possible to calibrate the effective discriminant parameters for these different regions, so that an event from any such area can be incorporated into a unified database.

Events studied are the U.S. PNE's and earthquakes in the Colorado Plateau/Rockies region, explosions at the Kazakh (CIS) and Lop Nor (PRC) test sites, as well as earthquakes in and around this region of Asia. The discriminants being used here are the ratio of integrated short-period P-wave to long-period energy (predominantly surface wave) summed over the three components (sp_z-P/lp_3) (Woods and Helmberger, 1994), the ratio of integrated short-period vertical component energy between the P and S wavetrains (sp_z-P/sp_z-S), and the ratio of M_L to scalar seismic moment (M_0), M_L:M_0 (Woods *et al*, 1994).

The energy ratio discriminants are empirical and only require the velocity records, whereas the M_L:M_0 discriminant is deterministic in that it involves waveform inversion for source parameters, which in turn requires establishing crustal models for these regions. Besides being used for source inversion, such Green's functions can be used to calibrate paths with respect to specific regional phases used for magnitude measurements and other discriminants. This study is primarily concerned with calibrating the regional crustal structure centered about the station WMQ in central Asia, and the region encompassing Pakistan and eastern Iran. These path calibrations are particularly useful for regions where no large explosions have taken place, as it is then possible to predict waveforms for such sources, thus helping to establish criterion for a "first-blast" in the region.

These discriminants and waveform modeling techniques have an effective threshold at or above M_L=4, for regional events, so that they fit the monitoring criteria of the CTBT.

RESEARCH ACCOMPLISHED:

Figure 1 plots the sp_z-P/lp_3 integrated energy ratio vs. distance for central Asian events. Explosions are circles and earthquakes are crosses, and each datum point represents one station - event pair. This method yields good separation of the two populations. Note also the Ural event (triangles) which plots in the earthquake population. It is now believed that this event was a mine collapse. More explosion data at a range of distances would help to establish the efficacy of this discriminant. In comparing these results to the original study (Woods and Helmberger, 1994) using regional TERRAscope data, we find that earthquakes and explosions demonstrate the same trends in Asia as they do in North America, although several Asian earthquakes near 500 km do have relatively high sp_z-P/lp_3 ratios. The Asian explosions also plot fairly high, suggesting the the regional crustal structure and Q may be responsible for these differences by increasing the relative high-frequency content of the wavefield.

This discriminant was also applied to events in the Colorado Plateau - Rocky Mountain region, hereafter referred to as the Colorado data. Source information for these events is given in table 1. The data obtained was primarily from WWSN analog records. The short-period records are of generally low quality, so that they could not be digitized. So instead of calculating the integrated energy, the peak short-period P-wave amplitude was taken, as well as the sum of the peak amplitude of the three long-period components. Figure 2 is the plot of the ratio of short-period P-wave amplitude to the sum of the three long-period components vs.

distance. For this version of the discriminant, the two source type populations also have different trending data, although there is some overlap. The fact this alternate method works makes it a promising discriminant to use on historical analog data, of even poor visual quality, to calibrate the sp_z-P/lp_3 ratio vs. distance for regions with sparse modern data coverage. In the original study of TERRAscope data (Woods and Helmberger, 1994), it was found that peak amplitude measurements worked nearly as well as integrated energy at discriminating events.

Another promising empirical discriminant is the ratio of integrated sp_z-P/sp_z-S. Figure 3 plots this ratio vs. distance for Asian events. Each datum point represents one station - event pair. The populations are well separated, although, again the data sets are too small to make any firm conclusions. This time the Ural event plots in the explosion population. A similar discriminant had been applied to regional TERRAscope data, with poorer results, however the seismograms had not been narrow-band filtered. It is believed that this step significantly enhances the separation of source types. Waveforms for central Asian events display more high-frequency energy than do those in the Basin and Range and neighboring provinces. These observation has been reported by Given *et al* (1990) as well.

A modified, peak-amplitude version of the sp_z-P/sp_z-S was performed on the Colorado data, the results of which are shown in figure 4. Here, also, the two source-type populations are separated by this discriminant. This again suggests that the modified discriminant can be used to calibrate regional sp_z-P/sp_z-S ratios for regions without adequate digital data.

Another use of the sp_z-P/sp_z-S ratio is as depth discriminant. Deep events waveforms can appear explosion-like in that the body-waves have sharp onsets and surface waves generated are relatively small. Also deeper events often are relatively high-frequency rich, again making them look explosion-like by some criteria. These differences can be seen in figure 5 which compares velocity records of a shallow (d=15km) and a deep (d=135km) event recorded in Pakistan. Both events are recorded at nearly the same range. Body-waves for the shallow event (top set of traces) are quite small compared to the surface wave and coda wavetrain. The deep event has strong, high-frequency rich, body waves and virtually no long-period (T>4 sec) coda. The bottom figure plots the integrated energy for each component of the two events. A large proportion (35 to 50 %) of the total energy arrives within the P-wavetrain for the deep event, whereas less than 10 percent of the total energy of the shallow event arrives in this time. This difference is most evident on the vertical components. Without treating this event as a deep source, it well could be misidentified as an explosion using some discrimination criteria such as m_b:MsubsS.

Using regional M_0 lowers the long-period measurement threshold to m_b=4, which is also near the threshold for teleseismic m_b measurements. Figure 6 plots M_L vs. M_0 for events in central Asia. Moments have been determined by us as well as taken from other studies, while M_L's have been taken from such studies or from bulletins where available.

We are also studying the area encompassing Pakistan and eastern Iran, see figure 7. As there are no large explosions recorded in this region, emphasis has been placed on broadband waveform modeling of the crustal structure instead. By modeling and understanding the propagational characteristics of a region using available earthquake data, one will be able to identify anomalous events when they do occur. As an example, figure 8 shows records from two stations of an event in Pakistan. The records are played-out as broadband displacement, under which are succeedingly higher bandpasses of the same record. In the bottom set of tangential traces, vertical bars have been placed just to the left of the Pn and Sn arrival times. At higher frequencies these phases become quite prominent. Typically the broadband record or even a longer-period waveform would be used to model this path. Secondary modeling of Q would be achieved by fitting the amplitude or energy of the high-frequency waveforms. Thus the path can be calibrated for both long- and short-period data.

To model waveforms one needs constraints on the sources. To this end, events were first inverted for the source mechanism using Green's functions developed for the Tibetan Plateau (TB) (Zhu and Helmberger, 1995; elsewhere in these proceedings). This model has a thick crust like that which is believed to underlie this mountainous region of Pakistan. The "cut and paste" method of inverting seismograms (Zhao and Helmberger, 1994), by fitting the Pnl and surface wavetrains separately, makes it possible to obtain good source inversions without requiring the use of a crustal model that correctly predicts the relative arrival time between the body waves and the surface waves. Figure 9 show array data and synthetic fits for one event (d=20km) using the inverted source parameters and the TB model. All waveforms have been low-pass filtered at 0.1 Hz. The first two columns of traces are the Pnl windows (Z and R, respectively), while the last three columns are for the surface waves (Z, R and T, respectively). The waveform fits are good for the body waves and surface waves. The number below each set of traces is the time shift of the data to synthetic, with a positive number indicating the synthetic being too fast by that amount. The source mechanism obtained also agrees with that for the Harvard CMT solution. The CMT solution places the depth at 44km. We found a depth of 20 km by cycling through Green's functions for the least-error inversion. As found in an earlier study by Zhao and Helmberger (1993) most crustal events are shallower than generally reported in this region of thickened crust as determined from teleseismic depth phases. Figure 10 shows fits of the array data for a deep (d=139) event. Again the waveform fits are good. Thus we have been successful in modeling both crustal and deep earthquakes. The next step is to refine the crustal structure by modeling the broadband waveforms of events for which their long-period source mechanism has been obtained.

CONCLUSIONS AND RECOMMENDATIONS:

All the discriminants discussed above all show promise with the Asian and Colorado data sets. The success of the narrow-band sp_z-P/sp_z-S ratio suggests that narrower-band measurements for any empirical discriminants may be in order. This passband will be applied to TERRAscope sp_z-P/sp_z-S data to compare with that for Asia. Furthermore this energy ratio can be used to identify deep events where there is such seismicity. Analysis of the Ural mine collapse using these discriminants suggests that it was rich in long-period energy and deficient in shear-wave energy. The success of modeling regional deep events with fairly simple 1-D crustal models suggests that it will be possible to accurately determine teleseismic t^* for such regions. One can obtain the source time function and other source parameters from regional data. With these parameters known, one can then match teleseismic records by varying t^*, thus calibrating m_b measurements for the region. Moreover, we can probably calibrate far regional data, upper-mantle phases, and perform joint source inversions to help resolve events poorly constrained in depth and origin time by using depth phases.

REFERENCES:

Given, H. K., N. Tarasov, V. Zhuravlev, F. L. Vernon, J. Berger, and I. L. Nersesov, 1990. High-Frequency Seismic Observations in Eastern Kazakhstan, USSR, with Emphasis on Chemical Explosion Experiments, *J. Geophys. Res.*, **95**, pp. 295-307.

Woods, B. B., S. Kedar, and D. V. Helmberger, 1993. M_L:M_0 as a Regional Seismic Discriminant, *Bull. Seism. Soc. Am.*, **83**, pp. 1167-1183.

Woods, B. B. and D. V. Helmberger, 1994. Regional Seismic Discriminants Using Wavetrain Energy Ratios, submitted to *Bull. Seism. Soc. Am.*

Zhao, L. Z. and D. V. Helmberger, 1993. Geophysical Implication from Relocations of Tibetan Earthquakes - Hot Lithosphere, *Geophys. Res. Let.* **18** pp.2205-2208.

Zhao, L. Z. and D. V. Helmberger, 1994. Source Estimation from Broadband Regional Seismograms, *Bull. Seism. Soc. Am.*, **84**, pp. 91-104

Zhu, L. and D. V. Helmberger, 1995. Intermediate Depth Earthquakes beneath the India-Tibet Collision Zone, submitted to *Geophys. Res. Let.*

Table 1:

U.S. PNE's and nearby earthquakes studied					
Event	Date	Time	Lat.	Lon.	m_b
GNOME	61/12/10	19:00	32.26	-103.87	-
GASBUGGY	67/12/10	19:30	36.7	-107.2	5.1
RULISON	70/08/28	21:00	39.4	-107.9	5.3
Colorado EQ	66/01/05	00:37	39.8	-104.7	5.0
Colorado EQ	67/08/09	12:25	39.9	-104.7	5.3
N. Mexico EQ	66/01/23	01:56	37.0	-107.0	5.5
N. Mexico AS	66/01/23	06:14	"	"	4.3
N. Mexico AS	66/01/23	07:49	"	"	4.6
N. Mexico AS	66/01/23	11:01	"	"	4.3
N. Mexico AS	66/01/23	19:43	36.9	-107.1	4.5
N. Mexico AS	66/01/23	23:48	36.9	-107.0	4.6

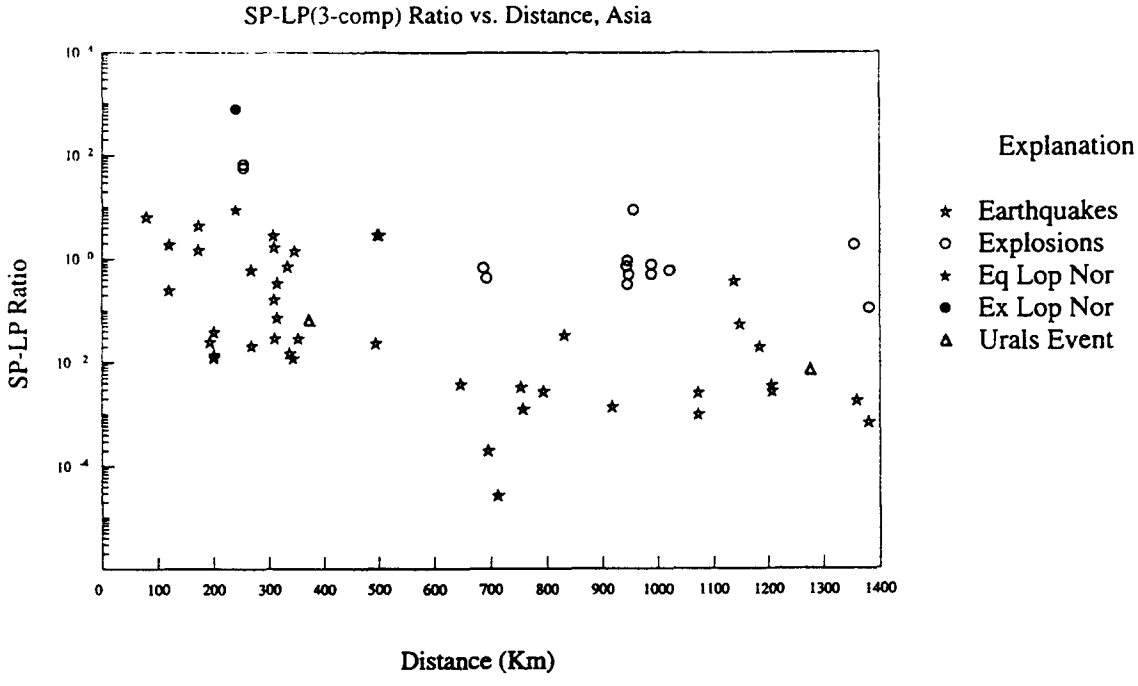

Figure 1. sp_z-P/lp_3 vs. distance for events in Asia. Explosions are circles, stars are earthquakes, and triangles represent the Ural mine collpase.

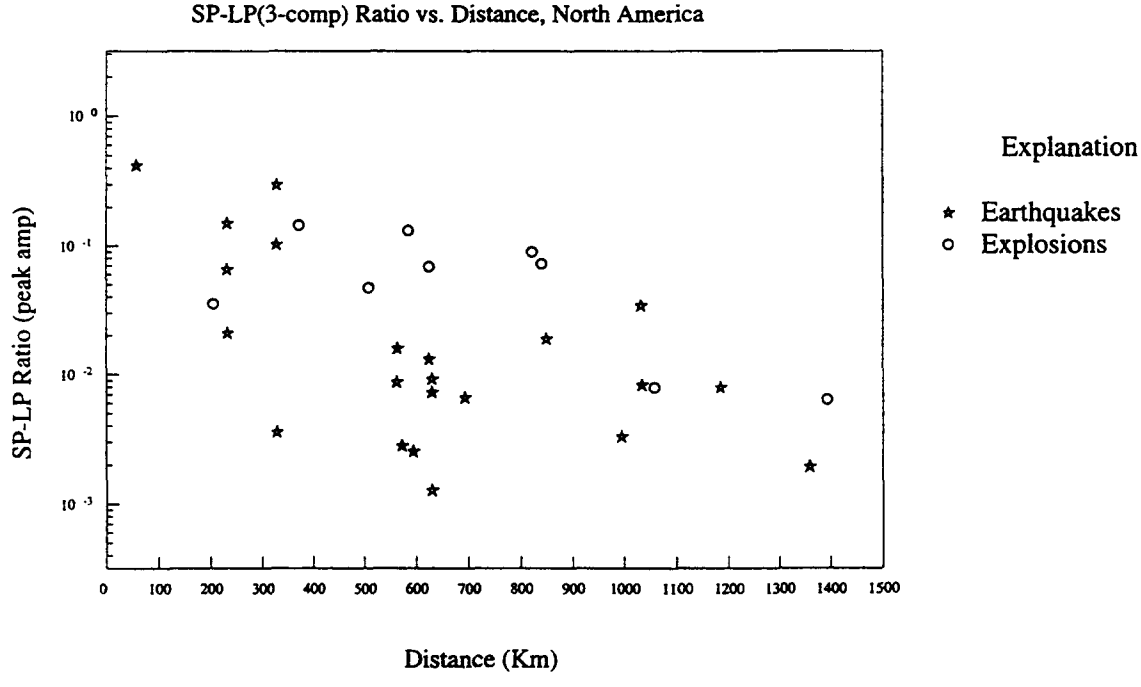

Figure 2. sp_z-P(peak amp.)/lp_3(peak amp) vs. distance for events in the Colorado Plateau region. Explosions are circles and stars are earthquakes.

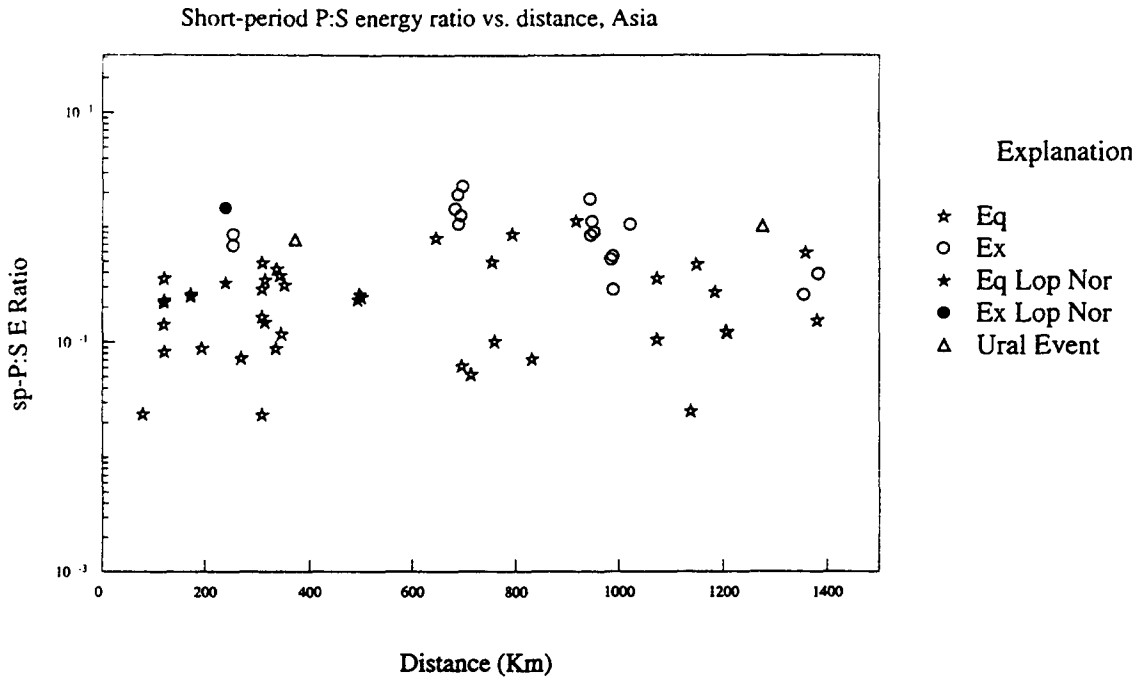

Figure 3. sp_z-P/sp_z-S energy ratio vs. distance for the Lop Nor and Kazakh explosions and nearby earthquakes.

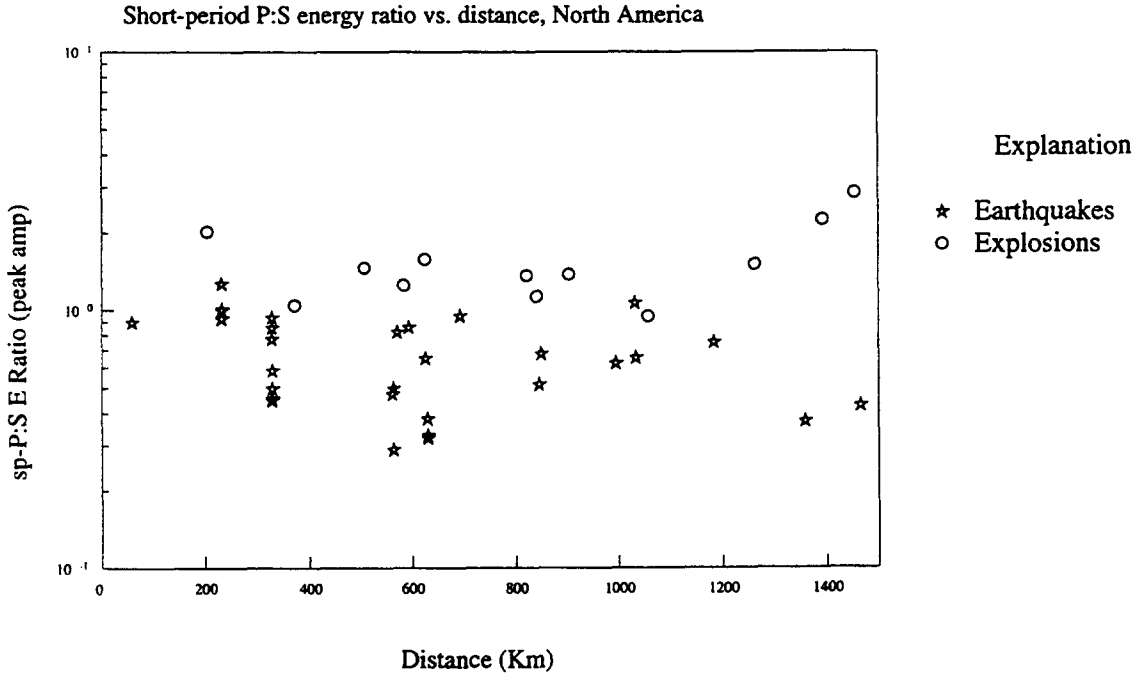

Figure 4. sp_z-P/sp_z-S energy ratio vs. distance for the U.S. PNE's and nearby earthquakes.

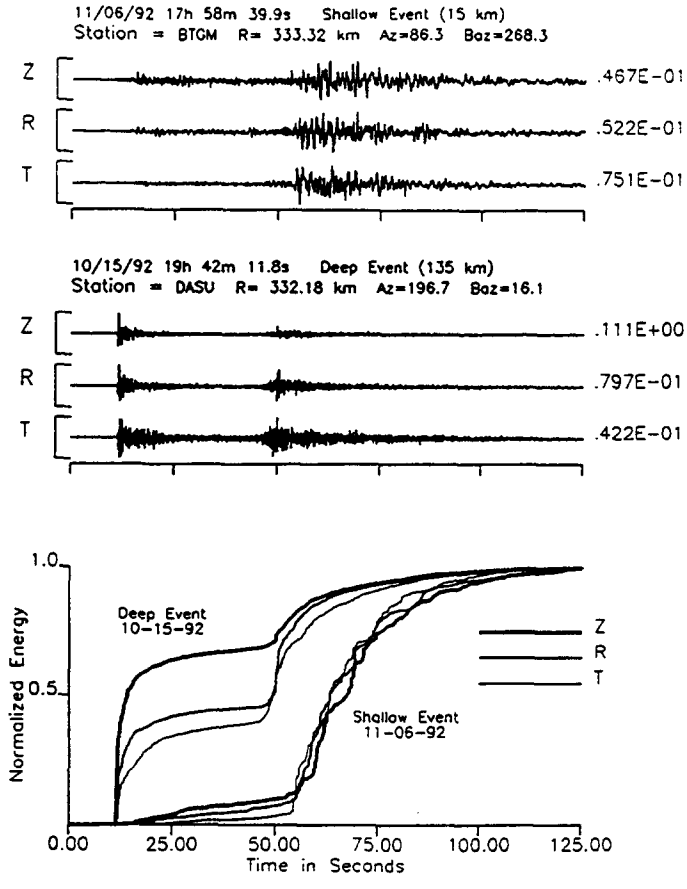

Figure 5. Broadband velocity records for a shallow event (top traces) and a deep event (middle traces) recorded by the Pakistan PASCAL array. The botttom figure plots the integrated energy curves for these records.

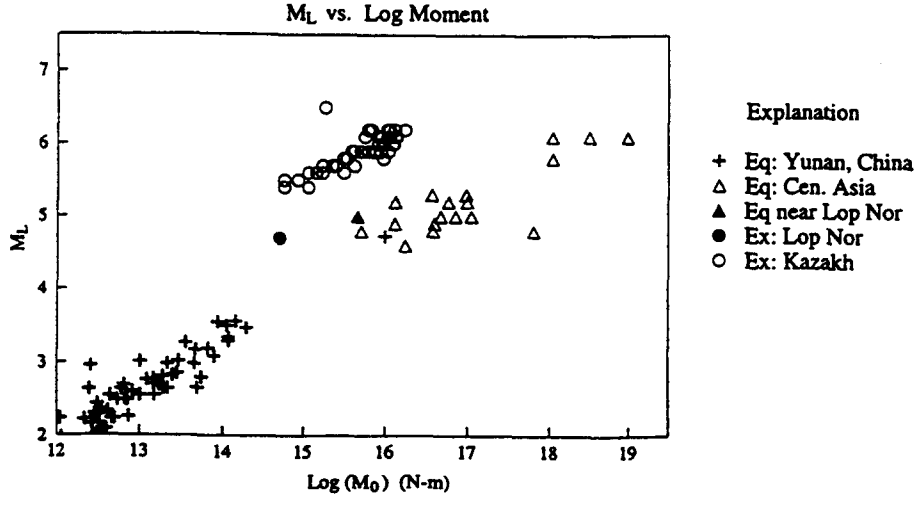

Figure 6. M_L vs. M_0 for Eurasian events.

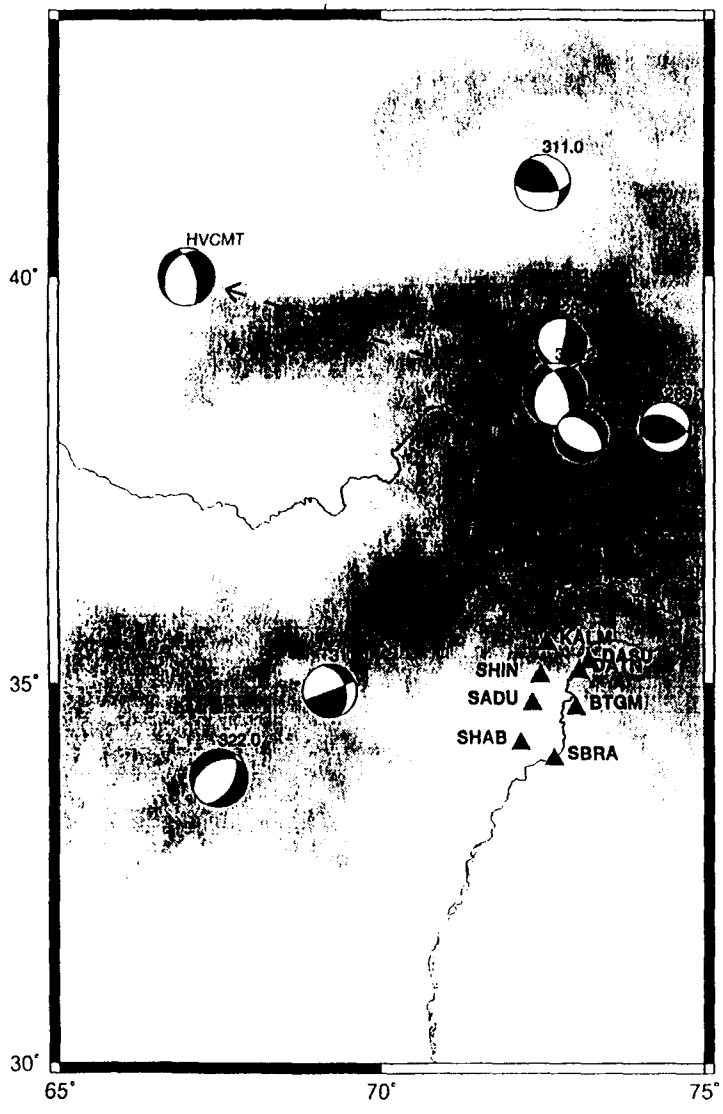

Figure 7. Map of Pakistan/eastern Iran study area and events studied. The Harvard CMT solution is for the event 328.2.

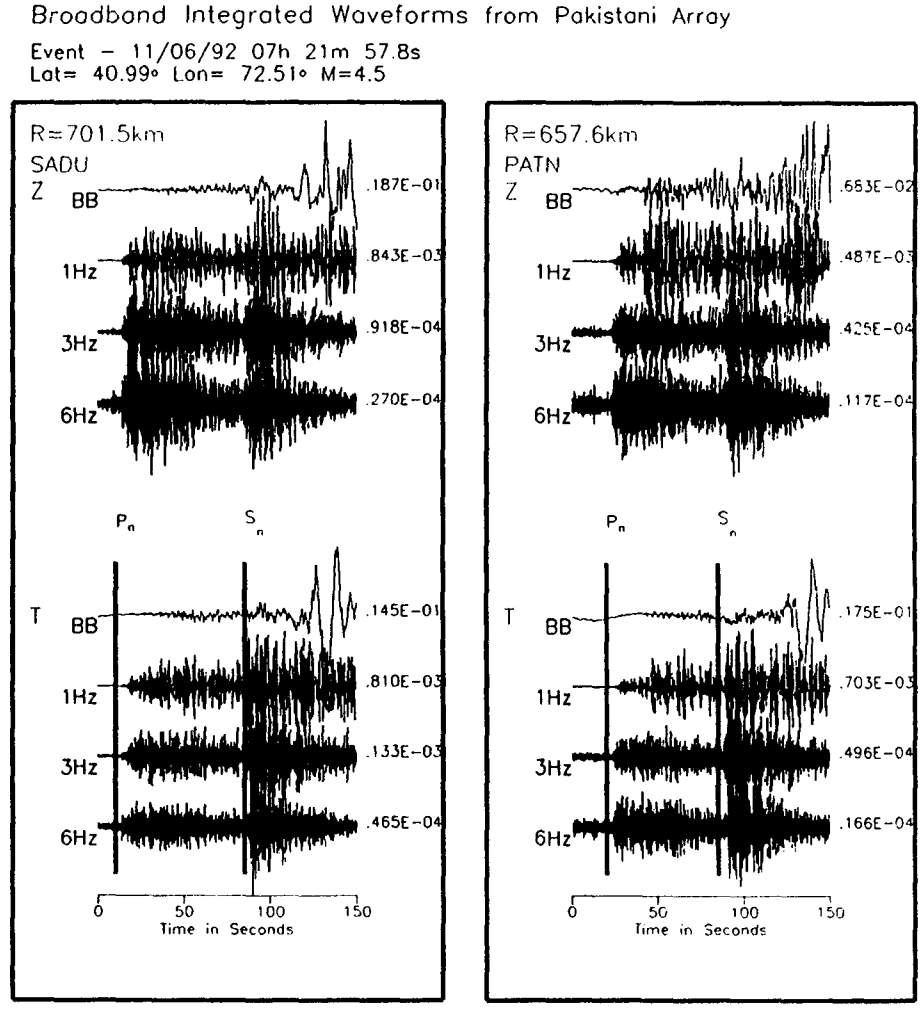

Figure 8. Regional wavefroms from Pakistan played-out at different different bandwidths.

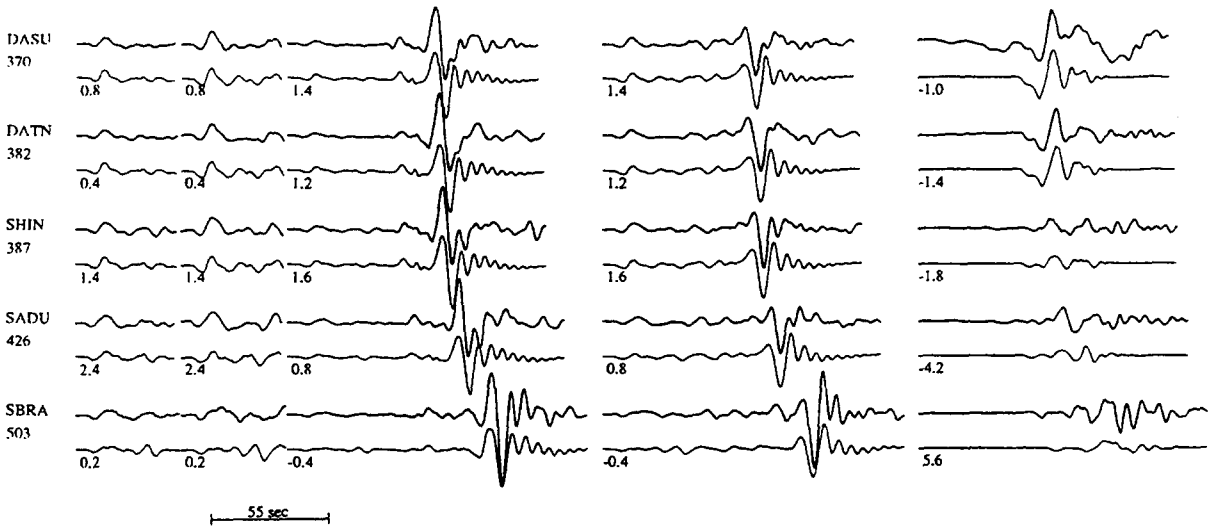

Figure 9. Data to synthetic waveform comparisons for the inversion of event 328.2 (240,60,240; M_w=6.0; d=20km). The data is the top, heavier trace. The number below the trace is the time-shift of the synthetic, with positive numbers indicating fast synthetics.

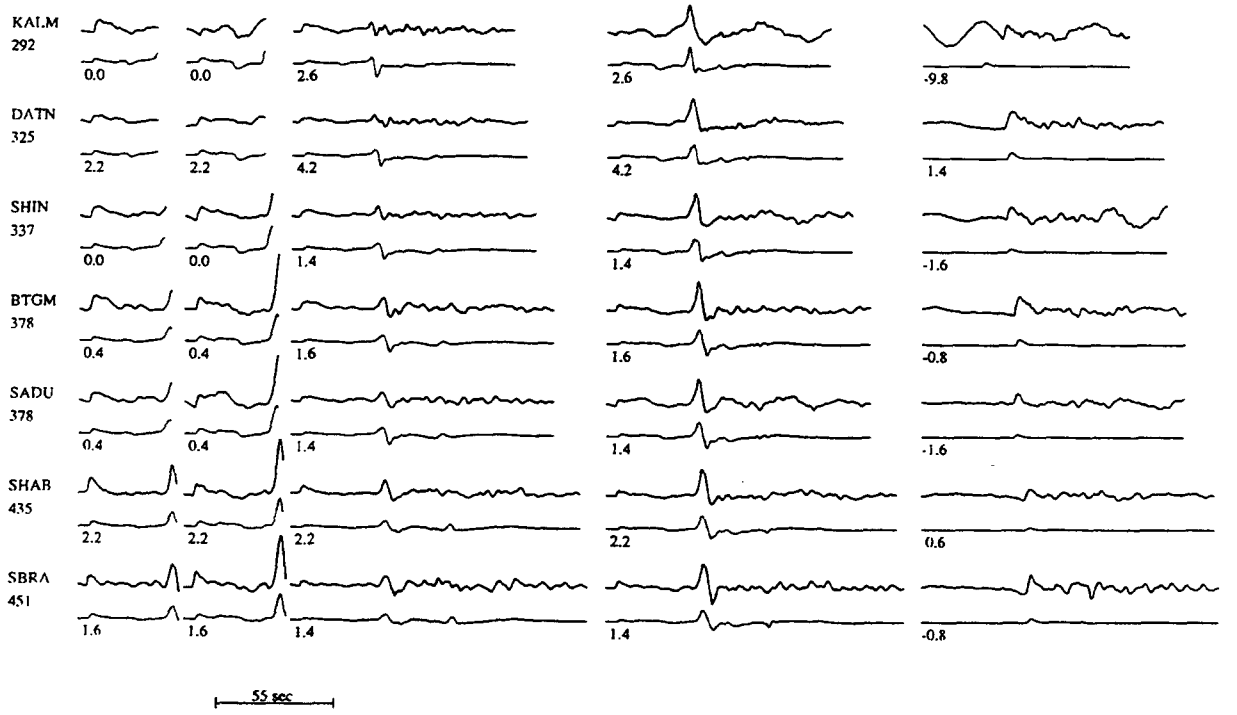

Figure 10. Data to synthetic waveform comparisons for the inversion of event 276.1 (110,50,270; M_w=5.1; d=150km).